Published in final edited form as:
J Nucl Med. 2011 April ; 52(4): 608–616. doi:10.2967/jnumed.110.086009.

Effects of the Amino Acid Linkers on the Melanoma-Targeting and Pharmacokinetic Properties of Indium-111-labeled Lactam Bridge-Cyclized α-MSH Peptides

Haixun Guo[1], **Jianquan Yang**[1], **Fabio Gallazzi**[4], and **Yubin Miao**[1,2,3]

[1]College of Pharmacy, University of New Mexico, Albuquerque, NM 87131, USA

[2]Cancer Research and Treatment Center, University of New Mexico, Albuquerque, NM 87131, USA

[3]Department of Dermatology, University of New Mexico, Albuquerque, NM 87131, USA

[4]Department of Biochemistry, University of Missouri, Columbia, MO 65211, USA

Abstract

The purpose of this study was to examine the profound effects of the amino acid linkers on the melanoma targeting and pharmacokinetic properties of novel ^{111}In-labeled lactam bridge-cyclized DOTA-[X]-CycMSH$_{hex}$ {1,4,7,10-Tetraazacyclododecane-1,4,7,10-tetraacetic acid-[X]-c[Asp-His-$_D$Phe-Arg-Trp-Lys]-CONH$_2$, X=GlyGlyNle, GlyGluNle or NleGlyGlu} peptides.

Methods—Three novel DOTA-GGNle-CycMSH$_{hex}$, DOTA-GENle-CycMSH$_{hex}$ and DOTA-NleGE-CycMSH$_{hex}$ peptides were designed and synthesized. The melanocortin-1 (MC1) receptor binding affinities of the peptides were determined in B16/F1 melanoma cells. The melanoma targeting and pharmacokinetic properties of ^{111}In-DOTA-GGNle-CycMSH$_{hex}$ and ^{111}In-DOTA-GENle-CycMSH$_{hex}$ were determined in B16/F1 melanoma-bearing C57 mice.

Results—DOTA-GGNle-CycMSH$_{hex}$ and DOTA-GENle-CycMSH$_{hex}$ displayed 2.1 and 11.5 nM MC1 receptor binding affinities, whereas DOTA-NleGE-CycMSH$_{hex}$ showed 873.4 nM MC1 receptor binding affinity. The introduction of the -GlyGly- linker maintained high melanoma uptake while decreased the renal and liver uptakes of ^{111}In-DOTA-GlyGlyNle-CycMSH$_{hex}$. The tumor uptake values of ^{111}In-DOTA-GGNle-CycMSH$_{hex}$ were 19.05 ± 5.04 and 18.6 ± 3.56 % injected dose/gram (%ID/g) at 2 and 4 h post-injection. ^{111}In-DOTA-GGNle-CycMSH$_{hex}$ exhibited 28, 32 and 42% less renal uptake values than ^{111}In-DOTA-Nle-CycMSH$_{hex}$ we reported previously, and 61, 65 and 68% less liver uptake values than ^{111}In-DOTA-Nle-CycMSH$_{hex}$ at 2, 4 and 24 h post-injection, respectively.

Conclusion—The amino acid linkers exhibited the profound effects on the melanoma targeting and pharmacokinetic properties of the ^{111}In-labeled lactam bridge-cyclized α-MSH peptides. Introduction of the -GlyGly- linker maintained high melanoma uptake while reducing the renal and liver uptakes of ^{111}In-DOTA-GlyGlyNle-CycMSH$_{hex}$, highlighting its potential as an effective imaging probe for melanoma detection, as well as a therapeutic peptide for melanoma treatment when labeled with a therapeutic radionuclide.

Request for reprints: Yubin Miao, 2502 Marble NE, MSC09 5360, College of Pharmacy, University of New Mexico, Albuquerque, NM 87131. Phone: (505) 925-4437; Fax: (505) 272-6749; ymiao@salud.unm.edu.
First author: Haixun Guo, 2502 Marble NE, MSC09 5360, College of Pharmacy, University of New Mexico, Albuquerque, NM 87131. Phone: (505) 272-8034; Fax: (505) 272-6749; haguo@salud.unm.edu

Keywords

Alpha-melanocyte stimulating hormone; Radiolabeled cyclic peptide; Melanoma imaging

INTRODUCTION

Over the last decade, both radiolabeled linear and cyclized alpha-melanocyte stimulating hormone (α-MSH) peptides have been designed to target G protein-coupled melanocortin-1 (MC1) receptors (1–5) for melanoma radioimaging and radiotherapy (6–20). Due to the stabilization of secondary structures (i.e. beta turns), the cyclic peptides possess less conformational freedom and higher stabilities than the linear peptides. Furthermore, the stabilization of secondary structures makes the cyclic peptides better fit the receptor binding pocket, thus enhancing their receptor binding affinities. At the present time, disulfide bond, metal and lactam bridge have been successfully utilized to cyclize the radiolabeled α-MSH peptides (9–13,15–20). Among these cyclization strategies, metal and lactam bridge cyclization resulted in greater tumor uptake and lower renal uptake values of the radiolabeled α-MSH peptides than the disulfide bridge cyclization (12,13,15–20).

We have successfully developed a novel class of ^{111}In-labeled lactam bridge-cyclized DOTA-conjugated α-MSH peptides for primary and metastatic melanoma detection (15–19). Initially, a Lys-Asp lactam bridge was used to cyclize the MC1 receptor binding motif (His-$_D$Phe-Arg-Trp) to yield a 12-amino acid cyclic α-MSH peptide {CycMSH: c[Lys-Nle-Glu-His-$_D$Phe-Arg-Trp-Gly-Arg-Pro-Val-Asp]}. 1,4,7,10-Tetraazacyclododecane-1,4,7,10-tetraacetic acid (DOTA) was conjugated to the *N*-terminus of the CycMSH with or without an amino acid linker (-GlyGlu-) for radiolabeling. ^{111}In-DOTA-GlyGlu-CycMSH displayed high melanoma uptake (10.40 ± 1.40 % ID/g at 2 h post-injection) in B16/F1 melanoma-bearing C57 mice (15). Using ^{111}In-DOTA-GlyGlu-CycMSH as an imaging probe, both flank primary and pulmonary metastatic melanoma lesions could be clearly visualized by small animal single photon emission computed tomography (SPECT)/CT (15,16).

Recently, we have identified another novel DOTA-conjugated lactam bridge-cyclized α-MSH peptide with a 6-amino acid peptide ring {DOTA-Nle-CycMSH$_{hex}$: DOTA-Nle-c[Asp-His-$_D$Phe-Arg-Trp-Lys]-CONH$_2$} for melanoma targeting. The receptor binding motif of His-$_D$Phe-Arg-Trp was directly cyclized by an Asp-Lys lactam bridge. Interestingly, the reduction of the ring size dramatically enhanced the melanoma uptake (19.39 ± 1.65 % ID/g at 2 h post-injection) and reduced the renal uptake (9.52 ± 0.44 % ID/g at 2 h post-injection) of ^{111}In-DOTA-Nle-CycMSH$_{hex}$ compared to ^{111}In-DOTA-GlyGlu-CycMSH in B16/F1 melanoma-bearing C57 mice (15,19).

Hydrocarbon, amino acid and polyethylene glycol (PEG) linkers displayed profound favorable effects in the receptor binding affinities and pharmacokinetics of radiolabeled bombesin (21–25), RGD (26–29) and α-MSH peptides (15,16). To examine the effects of the amino acid linkers on melanoma targeting and pharmacokinetic properties, we designed three novel DOTA-conjugated lactam bridge-cyclized CycMSH$_{hex}$ peptides with different amino acid linkers in this study based on the unique structure of DOTA-Nle-CycMSH$_{hex}$ we previously reported (19). A neutral -Gly-Gly- (GG) linker and a negatively-charged -Gly-Glu- (GE) linker were inserted between the DOTA and Nle to generate DOTA-GGNle-CycMSH$_{hex}$ and DOTA-GENle-CycMSH$_{hex}$. Furthermore, the negatively-charged -Gly-Glu- linker was introduced between Nle and CycMSH$_{hex}$ to yield DOTA-NleGE-CycMSH$_{hex}$. The MC1 receptor binding affinities of these three peptides were determined in B16/F1 melanoma cells. Only DOTA-GGNle-CycMSH$_{hex}$ and DOTA-GENle-CycMSH$_{hex}$ displayed low nanomolar MC1 receptor binding affinities. Hence, we further determined the

melanoma targeting and pharmacokinetic properties of ^{111}In-DOTA-GGNle-CycMSH$_{hex}$ and ^{111}In-DOTA-GENle-CycMSH$_{hex}$ in B16/F1 melanoma-bearing C57 mice.

MATERIALS AND METHODS

Chemicals and Reagents

Amino acids and resin were purchased from Advanced ChemTech Inc. (Louisville, KY) and Novabiochem (San Diego, CA). DOTA-tri-t-butyl ester was purchased from Macrocyclics Inc. (Richardson, TX) for peptide synthesis. ^{125}I-Tyr^2-[Nle^4, $_D$-Phe^7]-α-MSH {^{125}I-(Tyr^2)-NDP-MSH} was obtained from PerkinElmer, Inc. (Waltham, MA) for in vitro receptor binding assay. $^{111}InCl_3$ was purchased from MDS Nordion, Inc. (Ottawa, ON, Canada) for radiolabeling. All other chemicals used in this study were purchased from Thermo Fischer Scientific (Waltham, MA) and used without further purification. B16/F1 murine melanoma cells were obtained from American Type Culture Collection (Manassas, VA).

Peptide Synthesis

New DOTA-GGNle-CycMSH$_{hex}$, DOTA-GENle-CycMSH$_{hex}$ and DOTA-NleGE-CycMSH$_{hex}$ peptides were synthesized using standard fluorenylmethyloxycarbonyl (Fmoc) chemistry according to our published procedure (19) with modifications. Briefly, linear peptide backbones of (tBu)$_3$DOTA-Gly-Gly-Nle-Asp(O-2-PhiPr)-His(Trt)-$_D$Phe-Arg(Pbf)-Trp(Boc)-Lys(Dde), (tBu)$_3$DOTA-Gly-Glu(OtBu)-Nle-Asp(O-2-PhiPr)-His(Trt)-$_D$Phe-Arg(Pbf)-Trp(Boc)-Lys(Dde) and (tBu)$_3$DOTA-Nle-Gly-Glu(OtBu)-Asp(O-2-PhiPr)-His(Trt)-$_D$Phe-Arg(Pbf)-Trp(Boc)-Lys(Dde) were synthesized on Sieber Amide resin by an Advanced ChemTech multiple-peptide synthesizer (Louisville, KY). Seventy micromoles of resin, 210 μmol of each Fmoc-protected amino acid and 210 μmol of (tBu)$_3$DOTA were used for the synthesis. The protecting group of Dde was removed by 2% hydrazine for peptide cyclization. The protecting group of 2-phenylisopropyl was removed and the protected peptide was cleaved from the resin treating with a mixture of 2.5% of trifluoroacetic acid (TFA) and 5% of triisopropylsilane. After the precipitation with ice-cold ether and characterization by liquid chromatography-mass spectroscopy (LC-MS), each protected peptide was dissolved in H_2O/CH_3CN (50:50) and lyophilized to remove the reagents. Then, each protected peptide was further cyclized by coupling the carboxylic group from the Asp with the epsilon amino group from the Lys. The cyclization reaction was achieved by an overnight reaction in dimethylformamide (DMF) using benzotriazole-1-yl-oxy-tris-pyrrolidino-phosphonium-hexafluorophosphate (PyBOP) as a coupling agent in the presence of N,N-diisopropylethylamine (DIEA). After the characterization by LC-MS, each cyclized protected peptide was dissolved in H_2O/CH_3CN (50:50) and lyophilized to remove the reagents. The protecting groups were totally removed by treating with a mixture of trifluoroacetic acid (TFA), thioanisole, phenol, water, ethanedithiol and triisopropylsilane (87.5:2.5:2.5:2.5:2.5:2.5) for 2 h at room temperature (25 °C). Each peptide was precipitated and washed with ice-cold ether four times, purified by reverse phase-high performance liquid chromatography (RP-HPLC) and characterized by LC-MS.

In vitro Receptor Binding Assay

The receptor binding affinities (IC_{50} values) of DOTA-GGNle-CycMSH$_{hex}$, DOTA-GENle-CycMSH$_{hex}$ and DOTA-NleGE-CycMSH$_{hex}$ were determined by *in vitro* competitive binding assay according to our published procedure (19) with modifications. B16/F1 cells in 24-well cell culture plates (5×10^5 cells/well) were incubated at room temperature (25°C) for 2 h with approximately 60,000 cpm of ^{125}I-Tyr^2-NDP-MSH in the presence of 10^{-12} to 10^{-5} M of each peptide in 0.3 mL of binding medium {Dulbecco's Modified Eagle's Medium with 25 mM *N*-(2-hydroxyethyl)-piperazine-*N*'-(2-ethanesulfonic acid), pH 7.4, 0.2% bovine serum albumin (BSA), 0.3 mM 1,10-phenathroline}. The medium was

aspirated after the incubation. The cells were rinsed twice with 0.5 mL of ice-cold pH 7.4, 0.2% BSA / 0.01 M phosphate buffered saline (PBS) and lysed in 0.5 mL of 1 N NaOH for 5 minutes. The activities associated with cells were measured in a Wallac 1480 automated gamma counter (PerkinElmer, Waltham, MA). The IC_{50} value of each peptide was calculated using Prism software (GraphPad Software, La Jolla, CA).

Peptide Radiolabeling with ^{111}In

Since DOTA-NleGE-CycMSH$_{hex}$ exhibited at least 78-fold lower receptor binding affinity than DOTA-GGNle-CycMSH$_{hex}$ and DOTA-GENle-CycMSH$_{hex}$, we only further evaluated DOTA-GGNle-CycMSH$_{hex}$ and DOTA-GENle-CycMSH$_{hex}$. ^{111}In-DOTA-GGNle-CycMSH$_{hex}$ and ^{111}In-DOTA-GENle-CycMSH$_{hex}$ were prepared in a 0.5 M NH_4OAc-buffered solution at pH 4.5 according to our published procedure (19). Briefly, 50 μL of $^{111}InCl_3$ (37–74 MBq in 0.05 M HCl aqueous solution), 10 μL of 1 mg/mL peptide aqueous solution and 400 μL of 0.5 M NH_4OAc (pH 4.5) were added into a reaction vial and incubated at 75°C for 45 mins. After the incubation, 10 μL of 0.5% EDTA (ethylenediaminetetraacetic acid) aqueous solution was added into the reaction vial to scavenge potential unbound $^{111}In^{3+}$ ions. The radiolabeled complexes were purified to single species by Waters RP-HPLC (Milford, MA) on a Grace Vydac C-18 reverse phase analytical column (Deerfield, IL) using the following gradient at a 1 mL/min flowrate. The mobile phase consisted of solvent A (20 mM HCl aqueous solution) and solvent B (100% CH_3CN). The gradient was initiated and kept at 82:18 A/B for 3 min followed by a linear gradient of 82:18 A/B to 72:28 A/B over 20 mins. Then, the gradient was changed from 72:28 A/B to 10:90 A/B over 3 min followed by an additional 5 min at 10:90 A/B. Thereafter, the gradient was changed from 10:90 A/B to 82:18 A/B over 3 mins. Each purified peptide sample was purged with N_2 gas for 20 min to remove the acetonitrile. The pH of the final solution was adjusted to 7.4 with 0.1 N NaOH and sterile saline for animal studies. *In vitro* serum stability of ^{111}In-DOTA-GGNle-CycMSH$_{hex}$ and ^{111}In-DOTA-GENle-CycMSH$_{hex}$ were determined by incubation in mouse serum at 37°C for 24 h and monitored for degradation by RP-HPLC.

Biodistribution Studies

All animal studies were conducted in compliance with Institutional Animal Care and Use Committee approval. The pharmacokinetics of ^{111}In-DOTA-GGNle-CycMSH$_{hex}$ and ^{111}In-DOTA-GENle-CycMSH$_{hex}$ were determined in B16/F1 melanoma-bearing C57 female mice (Harlan, Indianapolis, IN). The C57 mice were subcutaneously inoculated with 1×10^6 B16/F1 cells on the right flank for each mouse to generate B16/F1 melanomas. Ten days post inoculation, the tumor weights reached approximately 0.2 g. Each melanoma-bearing mouse was injected with 0.037 MBq of ^{111}In-DOTA-GGNle-CycMSH$_{hex}$ or ^{111}In-DOTA-GENle-CycMSH$_{hex}$ via the tail vein. Groups of 5 mice were sacrificed at 0.5, 2, 4 and 24 h post-injection, and tumors and organs of interest were harvested, weighed and counted. Blood values were taken as 6.5% of the whole-body weight. The specificities of the tumor uptake of ^{111}In-DOTA-GGNle-CycMSH$_{hex}$ and ^{111}In-DOTA-GENle-CycMSH$_{hex}$ were determined by co-injecting 10 μg (6.07 nmol) of unlabeled NDP-MSH which is a linear α-MSH peptide analogue with picomolar MC1 receptor binding affinity.

Melanoma Imaging

Since ^{111}In-DOTA-GGNle-CycMSH$_{hex}$ displayed more favorable tumor targeting and pharmacokinetic properties than ^{111}In-DOTA-GENle-CycMSH$_{hex}$, we only further evaluated the melanoma imaging property of ^{111}In-DOTA-GGNle-CycMSH$_{hex}$. One B16/F1 melanoma-bearing C57 mouse (10 days post the cell inoculation) was injected with 14.8 MBq of ^{111}In-DOTA-GGNle-CycMSH$_{hex}$ via the tail vein. The mouse was sacrificed for small animal SPECT/CT (Nano-SPECT/CT®, Bioscan) imaging at 2 h post-injection. The

CT imaging was immediately followed by the whole-body SPECT imaging. The SPECT scans of 24 projections were acquired. Reconstructed SPECT and CT data were visualized and co-registered using InVivoScope (Bioscan, Washington DC).

Metabolites of ^{111}In-DOTA-GGNle-CycMSH$_{hex}$ in Melanoma and Urine

Both melanoma and urine were collected from the mouse used for SPECT/CT imaging to analyze the metabolites of ^{111}In-DOTA-GGNle-CycMSH$_{hex}$ in melanoma and urine. The tumor was homogenized by a VWR homogenizer for 5 mins. Equal volume of ethanol was added into the tumor sample. The tumor sample was vortexed and then centrifuged at 16,000 g for 5 mins. The supernatant was transferred into a glass test tube and purged with N_2 gas for 20 min to remove the ethanol. Aliquots of the supernatant were injected into HPLC. The urinary sample was directly centrifuged at 16,000 g for 5 min prior to the HPLC analysis. Thereafter, aliquots of the urine were injected into HPLC. The HPLC gradient described above was used for the analyses of metabolites.

Statistical Analysis

Statistical analysis was performed using the Student's t-test for unpaired data. A 95% confidence level was chosen to determine the significant difference in tumor and renal uptakes between ^{111}In-DOTA-GGNle-CycMSH$_{hex}$ and ^{111}In-DOTA-GENle-CycMSH$_{hex}$, as well as the significant difference in tumor and renal uptakes between ^{111}In-DOTA-GGNle-CycMSH$_{hex}$ or ^{111}In-DOTA-GENle-CycMSH$_{hex}$ with/without NDP-MSH co-injection. The differences at the 95% confidence level ($p<0.05$) were considered significant.

RESULTS

Three novel α-MSH peptides, DOTA-GGNle-CycMSH$_{hex}$, DOTA-GENle-CycMSH$_{hex}$ and DOTA-NleGE-CycMSH$_{hex}$ were synthesized and purified by HPLC. All three peptides displayed greater than 95% purity after HPLC purification. The schematic structures of the peptides are shown in Figure 1. The identities of the peptides were confirmed by electrospray ionization mass spectrometry. The calculated and found molecular weights of the peptides are presented in Table 1. The receptor binding affinities of the peptides were determined in B16/F1 melanoma cells. The IC_{50} values of DOTA-GGNle-CycMSH$_{hex}$, DOTA-GENle-CycMSH$_{hex}$ and DOTA-NleGE-CycMSH$_{hex}$ were 2.1, 11.5 and 873.4 nM in B16/F1 cells, respectively (Table 1 and Fig. 2).

We only further evaluated DOTA-GGNle-CycMSH$_{hex}$ and DOTA-GENle-CycMSH$_{hex}$ since both peptides displayed low nanomolar MC1 receptor binding affinities. . DOTA-GGNle-CycMSH$_{hex}$ and DOTA-GENle-CycMSH$_{hex}$ were readily labeled with ^{111}In in 0.5 M ammonium acetate solution at pH 4.5 with greater than 95% radiolabeling yield. Each ^{111}In-labeled peptide was completely separated from its excess non-labeled peptide by RP-HPLC. The retention times of the peptides and their ^{111}In-labeled conjugates are showed in Table 1. The retention times of ^{111}In-DOTA-GGNle-CycMSH$_{hex}$ and ^{111}In-DOTA-GENle-CycMSH$_{hex}$ were 17.7 and 21.7 min, respectively. ^{111}In-DOTA-GGNle-CycMSH$_{hex}$ and ^{111}In-DOTA-GENle-CycMSH$_{hex}$ showed greater than 98% radiochemical purities after HPLC purification, and were stable in mouse serum at 37 °C for 24 h. Only intact ^{111}In-labeled conjugates were detected by RP-HPLC after 24 h of incubation in mouse serum.

We further evaluated the melanoma targeting and pharmacokinetic properties of ^{111}In-DOTA-GGNle-CycMSH$_{hex}$ and ^{111}In-DOTA-GENle-CycMSH$_{hex}$ in B16/F1 melanoma-bearing C57 mice. The biodistribution results of ^{111}In-DOTA-GGNle-CycMSH$_{hex}$ and ^{111}In-DOTA-GENle-CycMSH$_{hex}$ are shown in Table 2. ^{111}In-DOTA-GGNle-CycMSH$_{hex}$ exhibited rapid high melanoma uptake and prolonged tumor retention. The

tumor uptake value of ^{111}In-DOTA-GGNle-CycMSH$_{hex}$ was 18.39 ± 2.22 %ID/g at 0.5 h post-injection. The tumor uptake reached its peak value of 19.05 ± 5.04 % ID/g at 2 h post-injection. ^{111}In-DOTA-GGNle-CycMSH$_{hex}$ displayed similar high tumor uptake (18.6 ± 3.56 %ID/g) at 4 h post-injection. Even at 24 h post-injection, there was 6.77 ± 0.84 %ID/g of ^{111}In-DOTA-GGNle-CycMSH$_{hex}$ activity remained in the tumor. Approximately 98% of the tumor uptake of ^{111}In-DOTA-GGNle-CycMSH$_{hex}$ was blocked by 10 μg (6.07 nmol) of non-radiolabeled NDP-MSH ($p<0.05$), demonstrating that the tumor uptake was specific and MC1 receptor-mediated. Whole-body clearance of ^{111}In-DOTA-GGNle-CycMSH$_{hex}$ was rapid, with approximately 88.4% of the injected radioactivity cleared through the urinary system by 2 h post-injection. Normal organ uptakes of ^{111}In-DOTA-GGNle-CycMSH$_{hex}$ were low (<1.31% ID/g) except for the kidneys at 2, 4 and 24 h post-injection. The liver uptake of ^{111}In-DOTA-GGNle-CycMSH$_{hex}$ was less than 0.61 %ID/g at 2 h post-injection. The kidney uptake value was 15.19 ± 2.75 %ID/g at 0.5 h post-injection, and decreased to 6.84 ± 0.92 %ID/g at 2 h post-injection. Co-injection of NDP-MSH didn't significantly reduce the renal uptake of the ^{111}In-DOTA-GGNle-CycMSH$_{hex}$ activity at 2 h post-injection, indicating that the renal uptake was not MC1 receptor-mediated. High tumor uptake and prolonged tumor retention coupled with rapid whole-body clearance resulted in high tumor/blood and high tumor/normal organ uptake ratios that were achieved as early as 0.5 h post-injection. The tumor/liver uptake ratios of ^{111}In-DOTA-GGNle-CycMSH$_{hex}$ were 33.42 and 31.0 at 2 and 4 h post-injection, whereas the tumor/kidney uptake ratios of ^{111}In-DOTA-GGNle-CycMSH$_{hex}$ were 2.79 and 2.73 at 2 and 4 h post-injection.

As we anticipated, ^{111}In-DOTA-GENle-CycMSH$_{hex}$ showed lower tumor uptake values than ^{111}In-DOTA-GGNle-CycMSH$_{hex}$ at 0.5, 2 and 4 h post-injection. The tumor uptake values of ^{111}In-DOTA-GGNle-CycMSH$_{hex}$ were 2, 2.5 and 3 times the tumor uptake values of ^{111}In-DOTA-GENle-CycMSH$_{hex}$ at 0.5, 2 and 4 h post-injection, respectively (Table 2). Co-injection of non-radioactive NDP-MSH blocked 95.6% of the tumor uptake at 2 h post-injection ($p<0.05$), indicating that the tumor uptake of ^{111}In-DOTA-GENle-CycMSH$_{hex}$ was MC1 receptor-specific. Despite the similar renal uptake of ^{111}In-DOTA-GENle-CycMSH$_{hex}$ as ^{111}In-DOTA-GGNle-CycMSH$_{hex}$ at 2, 4 and 24 h post-injection, ^{111}In-DOTA-GENle-CycMSH$_{hex}$ showed 40% lower renal uptake than ^{111}In-DOTA-GGNle-CycMSH$_{hex}$ at 0.5 h post-injection ($p<0.05$). The kidney uptake of ^{111}In-DOTA-GENle-CycMSH$_{hex}$ was as low as 9.06 ± 2.20 %ID/g at 0.5 h post-injection and decreased to 5.54 ± 0.63 %ID/g at 2 h post-injection.

We further evaluated the melanoma imaging properties of ^{111}In-DOTA-GGNle-CycMSH$_{hex}$ since ^{111}In-DOTA-GGNle-CycMSH$_{hex}$ showed more favorable biodistribution properties than ^{111}In-DOTA-GENle-CycMSH$_{hex}$. The whole-body SPECT/CT images are presented in Figure 3. Flank melanoma tumors were clearly visualized by SPECT/CT using ^{111}In-DOTA-GGNle-CycMSH$_{hex}$ as an imaging probe. The whole-body images showed high tumor to normal organ uptake ratios except for the kidneys, which was consistent with the biodistribution results. Melanoma and urinary metabolites of ^{111}In-DOTA-GGNle-CycMSH$_{hex}$ were analyzed by RP-HPLC 2 h post-injection. Figure 4 illustrates both the HPLC profiles of melanoma and urine samples. ^{111}In-DOTA-GGNle-CycMSH$_{hex}$ remained intact in the both tumor and urine 2 h post-injection (Fig. 4).

DISCUSSION

We have been interested in developing lactam bridge-cyclized α-MSH peptides to target the MC1 receptors for melanoma detection (15–19). Unique lactam bridge-cyclization makes the cyclic α-MSH peptides resistant to proteolytic degradations in vivo, as well as provides the flexibility for fine structural modification (15,17,19). Recently, we have identified ^{111}In-DOTA-Nle-CycMSH$_{hex}$ with a 6-amino acid ring targeting the MC1 receptors for

melanoma imaging (19). Among these reported ^{111}In-labeled lactam bridge-cyclized α-MSH peptides (15,17,19), ^{111}In-DOTA-Nle-CycMSH$_{hex}$ displayed the highest melanoma uptake values (24.94 ± 4.58 %ID/g at 0.5 h post-injection and 19.39 ± 1.65 %ID/g at 2 h post-injection) in B16/F1 melanoma-bearing mice (19). The reduction of the ring size improved the tumor uptake and reduced the renal uptake of ^{111}In-DOTA-Nle-CycMSH$_{hex}$, providing a new insight into the design of novel lactam bridge-cyclized α-MSH peptides for melanoma targeting.

Hydrocarbon, amino acid and PEG linkers have been used to optimize the receptor binding affinities, as well as modifying the pharmacokinetic properties of radiolabeled bombesin (21–25), RGD (26–29) and α-MSH peptides (15,16). For instance, Volkert and colleagues reported that the hydrocarbon linkers ranging from 5-carbon to 8-carbon between the DOTA and bombesin peptide resulted in 0.6–1.7 nM receptor binding affinities for the DOTA-conjugated bombesin peptides. Either shorter or longer hydrocarbon linkers dramatically reduce the receptor binding affinity by 100-fold (21). Rogers and colleagues reported the profound effects of amino acid linkers (-GlyGlyGly-, -GlySerGly-, -GlySerSer- and -GlyGluGly-) between the DOTA and bombesin peptide on tumor and normal organ uptakes of the radiolabeled peptides (25). ^{64}Cu-labeled DOTA-conjugated bombesin peptide with the -GlyGlyGly- linker displayed the higher PC-3 tumor uptake, whereas the -GlySerGly- linker resulted in lower renal uptake (25). Recently, Liu and colleagues reported the improvement in tumor uptakes and pharmacokinetics of ^{64}Cu- and ^{99m}Tc-labeled cyclic RGD peptides using the -GlyGlyGly- and PEG4 linkers (26–29). We also demonstrated that the introduction of a negatively-charged -GlyGlu- linker enhanced the melanoma uptake and reduced the renal uptake of ^{111}In-DOTA-GlyGlu-CycMSH compared to ^{111}In-DOTA-CycMSH (15). Hence, we evaluated the effects of -GlyGly- and -GlyGlu- linkers on melanoma targeting and pharmacokinetic properties of ^{111}In-DOTA-[X]-CycMSH$_{hex}$ peptide constructs in this study.

DOTA-Nle-CycMSH$_{hex}$ displayed 1.8 nM MC1 receptor binding affinity in B16/F1 melanoma cells in our previous report (19). The MC1 receptor binding sequence of His-dPhe-Arg-Trp was directly cyclized by an Asp-Lys lactam bridge to generate the CycMSH$_{hex}$ moiety. The radiometal chelator DOTA was conjugated to the CycMSH$_{hex}$ moiety via a Nle to form DOTA-Nle-CycMSH$_{hex}$ peptide. Based on the unique structure of DOTA-Nle-CycMSH$_{hex}$, we initially introduced the amino acid linker (-GlyGlu-) between the DOTA and Nle or between the Nle and CycMSH$_{hex}$ moiety to determine which position was suitable for an amino acid linker. We found that the moiety of Nle-CycMSH$_{hex}$ was critical for maintaining the low nanomolar MC1 receptor binding affinity of the peptide. The introduction of the -GlyGlu- linker between the Nle and CycMSH$_{hex}$ moiety dramatically reduced the MC1 receptor binding affinity to 873.4 nM, whereas the introduction of the -GlyGlu- linker between the DOTA and Nle only decreased the MC1 receptor binding affinity to 11.5 nM. Interestingly, the -GlyGly- linker between the DOTA and Nle maintained the MC1 receptor binding affinity as 2.1 nM, further indicating that the moiety of Nle-CycMSH$_{hex}$ played a crucial role in maintaining the low nanomolar MC1 receptor binding affinity of the peptide. Furthermore, the amino acid between the DOTA and the moiety of Nle-CycMSH$_{hex}$ also showed a significant impact on the MC1 receptor binding affinity of the peptide. The neutral -GlyGly- linker was better than negatively-charged -GlyGlu- linker in terms of maintaining the low nanomolar MC1 receptor binding affinity of the peptide. The IC_{50} value of DOTA-GENle-CycMSH$_{hex}$ was 5.5 times the IC_{50} value of DOTA-GGNle-CycMSH$_{hex}$. It was likely that the electrostatic interaction between the negatively-charged Glu in the –GlyGlu- linker and the positively-charged Arg in the moiety of Nle-CycMSH$_{hex}$ affected the configuration of the MC1 receptor binding region (His-$_{D}$-Phe-Arg-Trp). The difference in MC1 receptor binding affinity between DOTA-GGNle-CycMSH$_{hex}$ and DOTA-GENle-CycMSH$_{hex}$ (2.1 nM vs. 11.5 nM) was also observed in the

difference in melanoma uptake between ^{111}In-DOTA-GGNle-CycMSH$_{hex}$ and ^{111}In-DOTA-GENle-CycMSH$_{hex}$ in B16/F1 melanoma-bearing C57 mice. The tumor uptake values of ^{111}In-DOTA-GGNle-CycMSH$_{hex}$ were 2, 2.5 and 3 times the tumor uptake values of ^{111}In-DOTA-GENle-CycMSH$_{hex}$ at 0.5, 2 and 4 h post-injection, respectively (Table 2). In our previous report, the introduction of a negatively-charged -GlyGlu- linker resulted in 44% lower renal uptake of ^{111}In-DOTA-GlyGlu-CycMSH at 4 h post-injection compared to ^{111}In-DOTA-CycMSH (15). In this study, ^{111}In-DOTA-GENle-CycMSH$_{hex}$ showed 40% lower renal uptake ($p<0.05$) than ^{111}In-DOTA-GGNle-CycMSH$_{hex}$ at 0.5 h post-injection (Table 2).

At the present time, the lactam bridge-cyclized ^{111}In-DOTA-Nle-CycMSH$_{hex}$ and the metal-cyclized ^{111}In-DOTA-Re(Arg^{11})CCMSH displayed the highest comparable melanoma uptakes among all reported ^{111}In-labeled linear and cyclic α-MSH peptides (13,19). The melanoma uptake values were 17.29 ± 2.49 and 17.41 ± 5.63 %ID/g at 2 and 4 h post-injection for ^{111}In-DOTA-Re(Arg^{11})CCMSH (13), whereas the melanoma uptake values were 19.39 ± 1.65 and 17.01 ± 2.54 %ID/g at 2 and 4 h post-injection for ^{111}In-DOTA-Nle-CycMSH$_{hex}$ (19). Meanwhile, ^{111}In-DOTA-Nle-CycMSH$_{hex}$ showed similar tumor/kidney uptake ratios as ^{111}In-DOTA-Re(Arg^{11})CCMSH at 2 and 24 h post-injection (19). In this study, the introduction of the -GlyGly- linker maintained high melanoma uptakes of ^{111}In-DOTA-GGNle-CycMSH$_{hex}$ (19.05 ± 5.04 and 18.6 ± 3.56 % ID/g at 2 and 4 h post-injection, respectively) compared to ^{111}In-DOTANle-CycMSH$_{hex}$, which was consistent with their similar MC1 receptor binding affinities (2.1 nM vs. 1.8 nM). Interestingly, the introduction of -GlyGly- linker reduced the liver and renal uptakes of ^{111}In-DOTA-GGNle-CycMSH$_{hex}$ compared to ^{111}In-DOTA-Nle-CycMSH$_{hex}$ (19). The reduction in liver and kidney uptakes might be attributed to the relatively faster whole-body clearance of ^{111}In-DOTA-GGNle-CycMSH$_{hex}$. Approximately 88% of ^{111}In-DOTA-GGNle-CycMSH$_{hex}$ activity cleared out of the body via urinary system at 2 h post-injection, whereas 82% of ^{111}In-DOTA-Nle-CycMSH$_{hex}$ activity washed out of the body via urinary tract at 2 h post-injection (19). ^{111}In-DOTA-GGNle-CycMSH$_{hex}$ exhibited 61, 65 and 68% less liver uptake values than ^{111}In-DOTA-Nle-CycMSH$_{hex}$ (Fig. 5), and 28, 32 and 42% less renal uptake values than ^{111}In-DOTA-Nle-CycMSH$_{hex}$ at 2, 4 and 24 h post-injection (Fig. 5), respectively. The maintained high melanoma uptakes coupled with the decreased liver and renal uptakes resulted in enhanced tumor/liver and tumor/kidney uptake ratios for ^{111}In-DOTA-GGNle-CycMSH$_{hex}$ compared to ^{111}In-DOTA-Nle-CycMSH$_{hex}$ at 2 and 4 h post-injection (Fig. 6). The tumor/liver uptake ratios of ^{111}In-DOTA-GGNle-CycMSH$_{hex}$ were 2.5 and 3.1 times the tumor/liver uptake ratios of ^{111}In-DOTA-Nle-CycMSH$_{hex}$ at 2 and 4 h post-injection, whereas the tumor/kidney uptake ratios of ^{111}In-DOTA-GGNle-CycMSH$_{hex}$ were 1.4 and 1.6 times the tumor/kidney uptake ratios of ^{111}In-DOTA-Nle-CycMSH$_{hex}$ at 2 and 4 h post-injection.

As showed in Fig. 3, the enhanced tumor/liver and tumor/kidney uptake ratios of ^{111}In-DOTA-GGNle-CycMSH$_{hex}$ generated high tumor imaging contrast to the background. The flank melanoma lesions were clearly visualized by SPECT/CT using ^{111}In-DOTA-GGNle-CycMSH$_{hex}$ as an imaging probe, highlighting its potential as an effective imaging agent for melanoma detection. ^{111}In-DOTA-GGNle-CycMSH$_{hex}$ maintained intact in melanoma and urine at 2 h post-injection (Fig. 4). From the therapeutic point of view, the enhanced tumor/liver and tumor/kidney uptake ratios of ^{111}In-DOTA-GGNle-CycMSH$_{hex}$ would decrease the absorbed doses to the liver and kidneys when using the therapeutic radionuclide-labeled DOTA-GGNle-CycMSH$_{hex}$ for melanoma treatment. In other words, the improvement of tumor/liver and tumor/kidney uptake ratios would potentially increase the absorbed dose to the tumor while keeping the liver and kidneys safe when treating the melanoma with the therapeutic radionuclide-labeled DOTA-GGNle-CycMSH$_{hex}$.

CONCLUSIONS

The amino acid linkers exhibited the profound effects on the melanoma targeting and pharmacokinetic properties of the ^{111}In-labeled lactam bridge-cyclized α-MSH peptides. Introduction of the -GlyGly- linker maintained high melanoma uptake while reducing the renal and liver uptakes of ^{111}In-DOTA-GlyGlyNle-CycMSH$_{hex}$, highlighting its potential as an effective imaging probe for melanoma detection, as well as a therapeutic peptide for melanoma treatment when labeled with a therapeutic radionuclide.

Acknowledgments

This work was supported by the NIH grant NM-INBRE P20RR016480. The image in this article was generated by the Keck-UNM Small Animal Imaging Resource established with funding from the W.M. Keck Foundation and the University of New Mexico Cancer Research and Treatment Center (NIH P30 CA118100).

REFERENCES

1. Siegrist W, Solca F, Stutz S, et al. Characterization of receptors for alpha-melanocyte-stimulating hormone on human melanoma cells. Cancer Res. 1989; 49:6352–6358. [PubMed: 2804981]
2. Tatro JB, Reichlin S. Specific receptors for alpha-melanocyte-stimulating hormone are widely distributed in tissues of rodents. Endocrinology. 1987; 121:1900–1907. [PubMed: 2822378]
3. Miao Y, Whitener D, Feng W, Owen NK, Chen J, Quinn TP. Evaluation of the human melanoma targeting properties of radiolabeled alpha-melanocyte stimulating hormone peptide analogues. Bioconjug Chem. 2003; 14:1177–1184. [PubMed: 14624632]
4. Miao Y, Owen NK, Whitener D, Gallazzi F, Hoffman TJ, Quinn TP. In vivo evaluation of ^{188}Re-labeled alpha-melanocyte stimulating hormone peptide analogs for melanoma therapy. Int J Cancer. 2002; 101:480–487. [PubMed: 12216078]
5. Chen J, Cheng Z, Hoffman TJ, Jurisson SS, Quinn TP. Melanoma-targeting properties of ^{99m}technetium-labeled cyclic alpha-melanocyte-stimulating hormone peptide analogues. Cancer Res. 2000; 60:5649–5658. [PubMed: 11059756]
6. Froidevaux S, Calame-Christe M, Tanner H, Eberle AN. Melanoma targeting with DOTA-alpha-melanocyte-stimulating hormone analogs: structural parameters affecting tumor uptake and kidney uptake. J Nucl Med. 2005; 46:887–895. [PubMed: 15872364]
7. Froidevaux S, Calame-Christe M, Schuhmacher J, et al. A gallium-labeled DOTA-alpha-melanocyte- stimulating hormone analog for PET imaging of melanoma metastases. J Nucl Med. 2004; 45:116–123. [PubMed: 14734683]
8. Froidevaux S, Calame-Christe M, Tanner H, Sumanovski L, Eberle AN. A novel DOTA-alpha-melanocyte-stimulating hormone analog for metastatic melanoma diagnosis. J Nucl Med. 2002; 43:1699–1706. [PubMed: 12468522]
9. Miao Y, Owen NK, Fisher DR, Hoffman TJ, Quinn TP. Therapeutic efficacy of a ^{188}Re-labeled alpha-melanocyte-stimulating hormone peptide analog in murine and human melanoma-bearing mouse models. J Nucl Med. 2005; 46:121–129. [PubMed: 15632042]
10. Miao Y, Hylarides M, Fisher DR, et al. Melanoma therapy via peptide-targeted alpha-radiation. Clin Cancer Res. 2005; 11:5616–5621. [PubMed: 16061880]
11. Wei L, Butcher C, Miao Y, et al. Synthesis and biologic evaluation of ^{64}Cu-labeled rhenium-cyclized alpha-MSH peptide analog using a cross-bridged cyclam chelator. J Nucl Med. 2007; 48:64–72. [PubMed: 17204700]
12. Miao Y, Benwell K, Quinn TP. ^{99m}Tc- and ^{111}In-labeled alpha-melanocyte-stimulating hormone peptides as imaging probes for primary and pulmonary metastatic melanoma detection. J Nucl Med. 2007; 48:73–80. [PubMed: 17204701]
13. Cheng Z, Chen J, Miao Y, Owen NK, Quinn TP, Jurisson SS. Modification of the structure of a metallopeptide: synthesis and biological evaluation of ^{111}In-labeled DOTA-conjugated rhenium-cyclized alpha-MSH analogues. J Med Chem. 2002; 45:3048–3056. [PubMed: 12086490]

14. Cheng Z, Xiong Z, Subbarayan M, Chen X, Gambhir SS. ^{64}Cu-labeled alpha-melanocyte-stimulating hormone analog for MicroPET imaging of melanocortin 1 receptor expression. Bioconjug Chem. 2007; 18:765–772. [PubMed: 17348700]
15. Miao Y, Gallazzi F, Guo H, Quinn TP. ^{111}In-labeled lactam bridge-cyclized alpha-melanocyte stimulating hormone peptide analogues for melanoma imaging. Bioconjug Chem. 2008; 19:539–547. [PubMed: 18197608]
16. Guo H, Shenoy N, Gershman BM, Yang J, Sklar LA, Miao Y. Metastatic melanoma imaging with an ^{111}In-labeled lactam bridge-cyclized alpha-melanocyte-stimulating hormone peptide. Nucl Med Biol. 2009; 36:267–276. [PubMed: 19324272]
17. Guo H, Yang J, Gallazzi F, Prossnitz ER, Sklar LA, Miao Y. Effect of DOTA position on melanoma targeting and pharmacokinetic properties of ^{111}In-labeled lactam bridge-cyclized α-melanocyte stimulating hormone peptide. Bioconjug Chem. 2009; 20:2162–2168. [PubMed: 19817405]
18. Guo H, Yang J, Shenoy N, Miao Y. Gallium-67-labeled lactam bridge-cyclized alpha-melanocyte stimulating hormone peptide for primary and metastatic melanoma imaging. Bioconjug Chem. 2009; 20:2356–2363. [PubMed: 19919057]
19. Guo H, Yang J, Gallazzi F, Miao Y. Reduction of the ring size of radiolabeled lactam bridge-cyclized alpha-MSH peptide resulting in enhanced melanoma uptake. J Nucl Med. 2010; 51:418–426. [PubMed: 20150256]
20. Chen J, Cheng Z, Owen NK, Hoffman TJ, Miao Y, Jurisson SS, Quinn TP. Evaluation of an ^{111}In-DOTA-rhenium cyclized α-MSH analog: a novel cyclic-peptide analog with improved tumor-targeting properties. J Nucl Med. 2001; 42:1847–1855. [PubMed: 11752084]
21. Hoffman TJ, Gali H, Smith CJ, Sieckman GL, Hayes DL, Owen NK, Volkert WA. Novel series of ^{111}In-labeled bombesin analogs as potential radiopharmaceuticals for specific targeting of gastrin-releasing peptide receptors expressed on human prostate cancer cells. J Nucl Med. 2003; 44:823–831. [PubMed: 12732685]
22. Garayoa EG, Schweinsberg C, Maes V, Brans L, Blauenstein P, Tourwe DA, Schibli R, Schbiger PA. Influence of the molecular charge on the biodistribution of bombesin analogues labeled with the [^{99m}Tc(CO)$_3$]-core. Bioconjug Chem. 2008; 19:2409–2416. [PubMed: 18998719]
23. Fragogeorgi EA, Zikos C, Gourni E, Bouziotis P, Paravatou-Petsotas M, Loudos G, Mitsokapas N, Xanthopoulos S, Mavri-Vavayanni M, Livaniou E, Varvarigou AD, Archimandritis SC. Spacer site modifications for the improvement of the *in vitro* and *in vivo* binding properties of ^{99m}Tc-N$_3$S-X-Bombesin[2–14] derivatives. Bioconjug Chem. 2009; 20:856–867. [PubMed: 19344122]
24. Garrison JC, Rold TL, Sieckman GL, Naz F, Sublett SV, Figueroa SD, Volkert WA, Hoffman TJ. Evaluation of the pharmacokinetic effects of various linking group using the ^{111}In-DOTA-X-BBN(7–14)NH$_2$ structural paradigm in a prostate cancer model. Bioconjug Chem. 2008; 19:1803–1812. [PubMed: 18712899]
25. Parry JJ, Kelly TS, Andrews R, Rogers BE. In vitro and in vivo evaluation of ^{64}Cu-labeled DOTA-Linker-Bombesin(7–14) analogues containing different amino acid linker moieties. Bioconjug Chem. 2007; 18:1110–1117. [PubMed: 17503761]
26. Liu S, He Z, Hsieh WY, Kim YS, Jiang Y. Impact of PKM linkers on biodistribution charateristics of the ^{99m}Tc-labeled cyclic RGDfK dimer. Bioconjug Chem. 2006; 17:1499–1507. [PubMed: 17105229]
27. Shi J, Wang L, Kim YS, Zhai S, Liu Z, Chen X, Liu S. Improving tumor uptake and excretion kinetics of ^{99m}Tc-labeled cyclic arginine-glycine-aspartic (RGD) dimers with triglycine linkers. J Med Chem. 2008; 51:7980–7990. [PubMed: 19049428]
28. Wang L, Shi J, Kim YS, Zhai S, Jia B, Zhao H, Liu Z, Wang F, Chen X, Liu S. Improving tumor-targeting capability and pharmacokinetics of ^{99m}Tc-labeled cyclic RGD dimers with PEG$_4$ linkers. Mol Pharm. 2009; 6:231–245. [PubMed: 19067525]
29. Shi J, Kim YS, Zhai S, Liu Z, Chen X, Liu S. Improving tumor uptake and pharmacokinetics of ^{64}Cu-labeled cyclic RGD peptide dimers with Gly$_3$ and PEG$_4$ linkers. Bioconjug Chem. 2009; 20:750–759. [PubMed: 19320477]

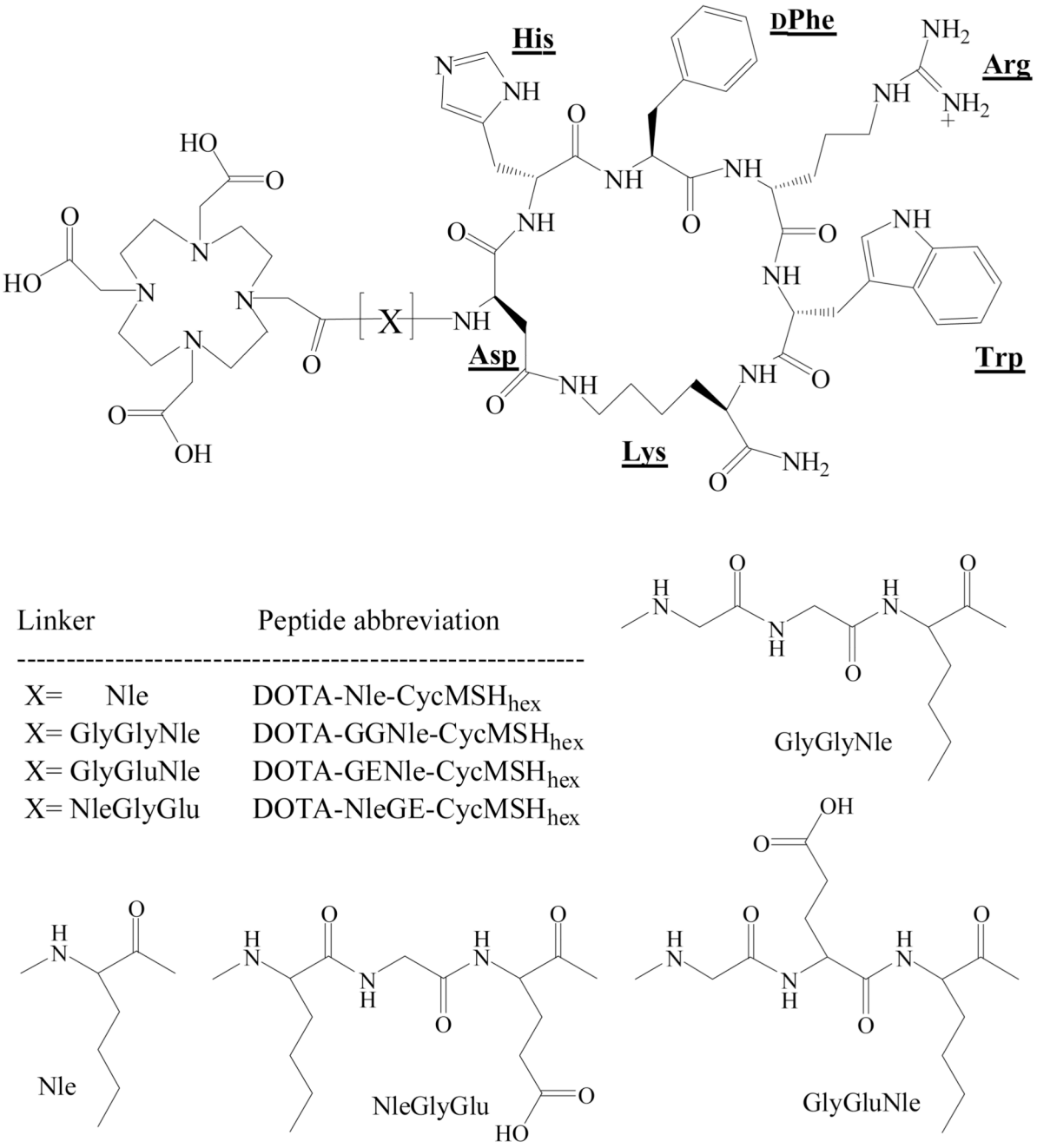

Figure 1.
Structures of DOTA-Nle-CycMSH$_{hex}$, DOTA-GGNle-CycMSH$_{hex}$, DOTA-GENle-CycMSH$_{hex}$ and DOTA-NleGE-CycMSH$_{hex}$. The structure of DOTA-Nle-CycMSH$_{hex}$ was cited from the reference [19] for comparison.

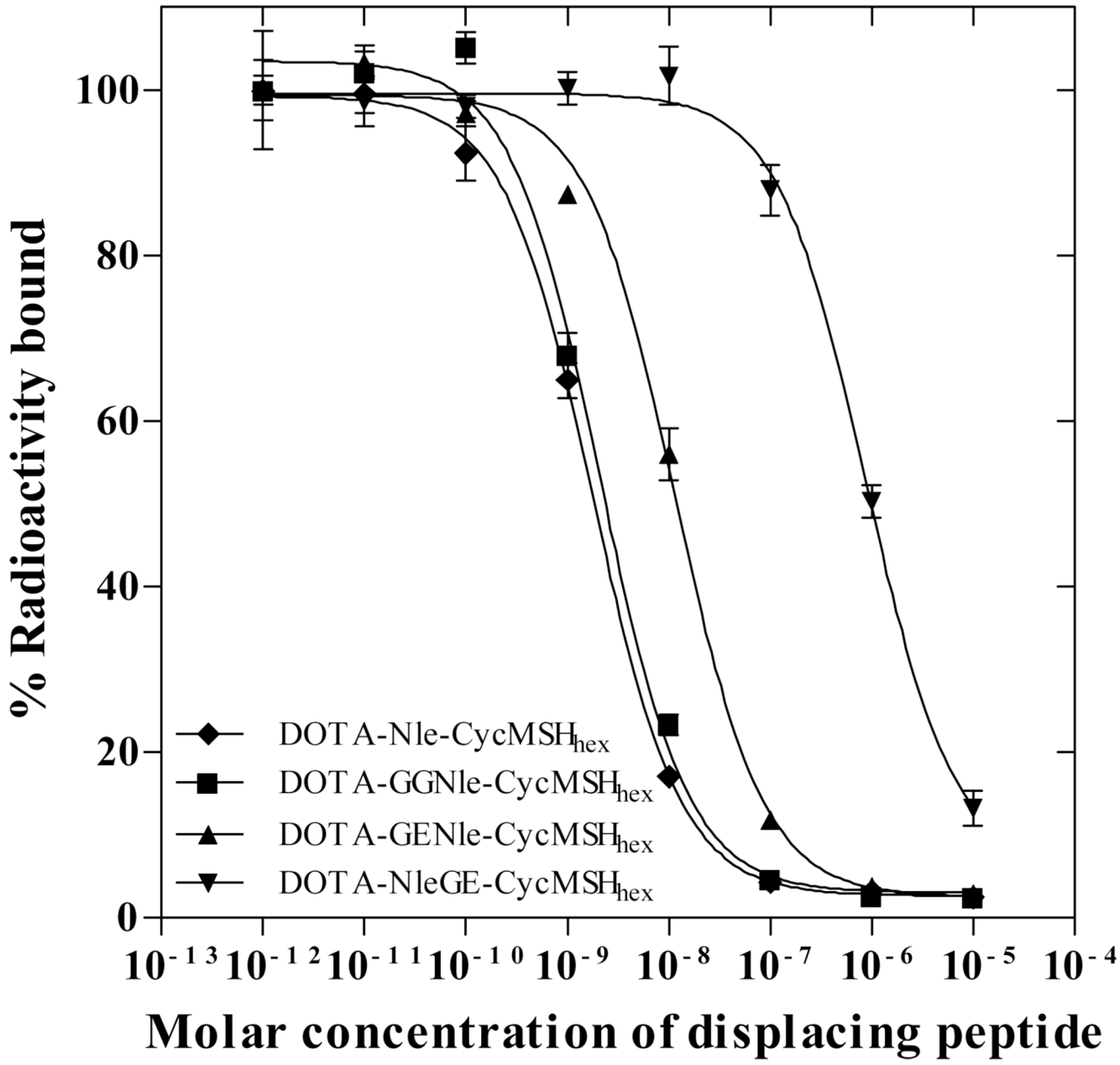

Figure 2.

The *in vitro* competitive binding curves of DOTA-Nle-CycMSH$_{hex}$, DOTA-GGNle-CycMSH$_{hex}$, DOTA-GENle-CycMSH$_{hex}$ and DOTA-NleGE-CycMSH$_{hex}$ in B16/F1 melanoma cells. The IC_{50} values of DOTA-Nle-CycMSH$_{hex}$, DOTA-GGNle-CycMSH$_{hex}$, DOTA-GENle-CycMSH$_{hex}$ and DOTA-NleGE-CycMSH$_{hex}$ were 1.8, 2.1, 11.5 and 873.4 nM respectively. The data of DOTA-Nle-CycMSH$_{hex}$ was cited from the reference [19] for comparison.

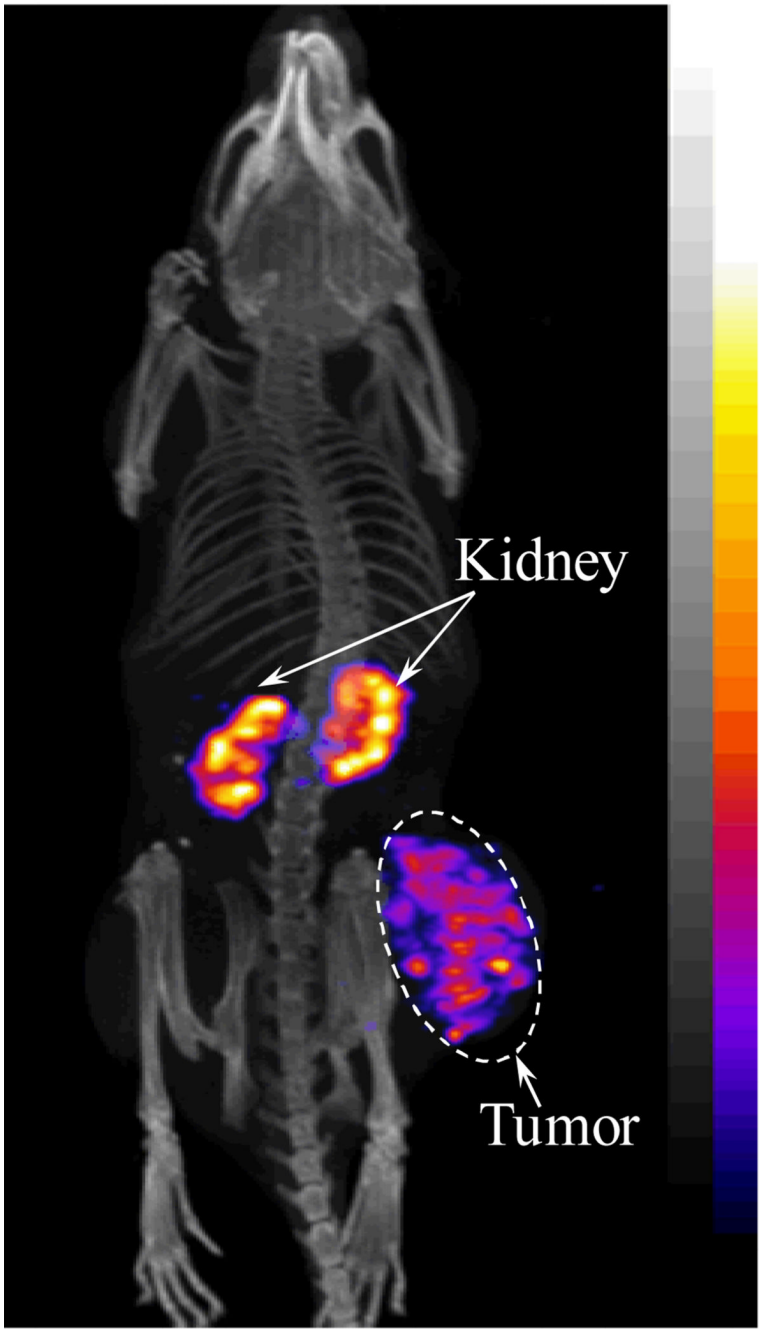

Figure 3.
Representative whole-body SPECT/CT images of a B16/F1 melanoma-bearing mouse (14 days post cell inoculation) at 2 h post-injection of 37.0 MBq of ^{111}In-DOTA-GGNle-CycMSH$_{hex}$.

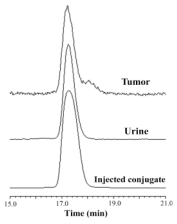

Figure 4.
Radioactive HPLC profiles of ^{111}In-DOTA-GGNle-CycMSH$_{hex}$ (injected conjugate) and its metabolites in urine and tumor at 2 h post-injection.

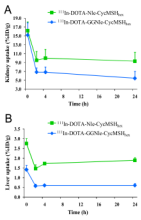

Figure 5.

The kidney (A) and liver (B) uptake values of ^{111}In-DOTA-Nle-CycMSH$_{hex}$ (■)and ^{111}In-DOTA-GGNle-CycMSH$_{hex}$ (◆). The data of ^{111}In-DOTA-Nle-CycMSH$_{hex}$ was cited from the reference [19] for comparison.

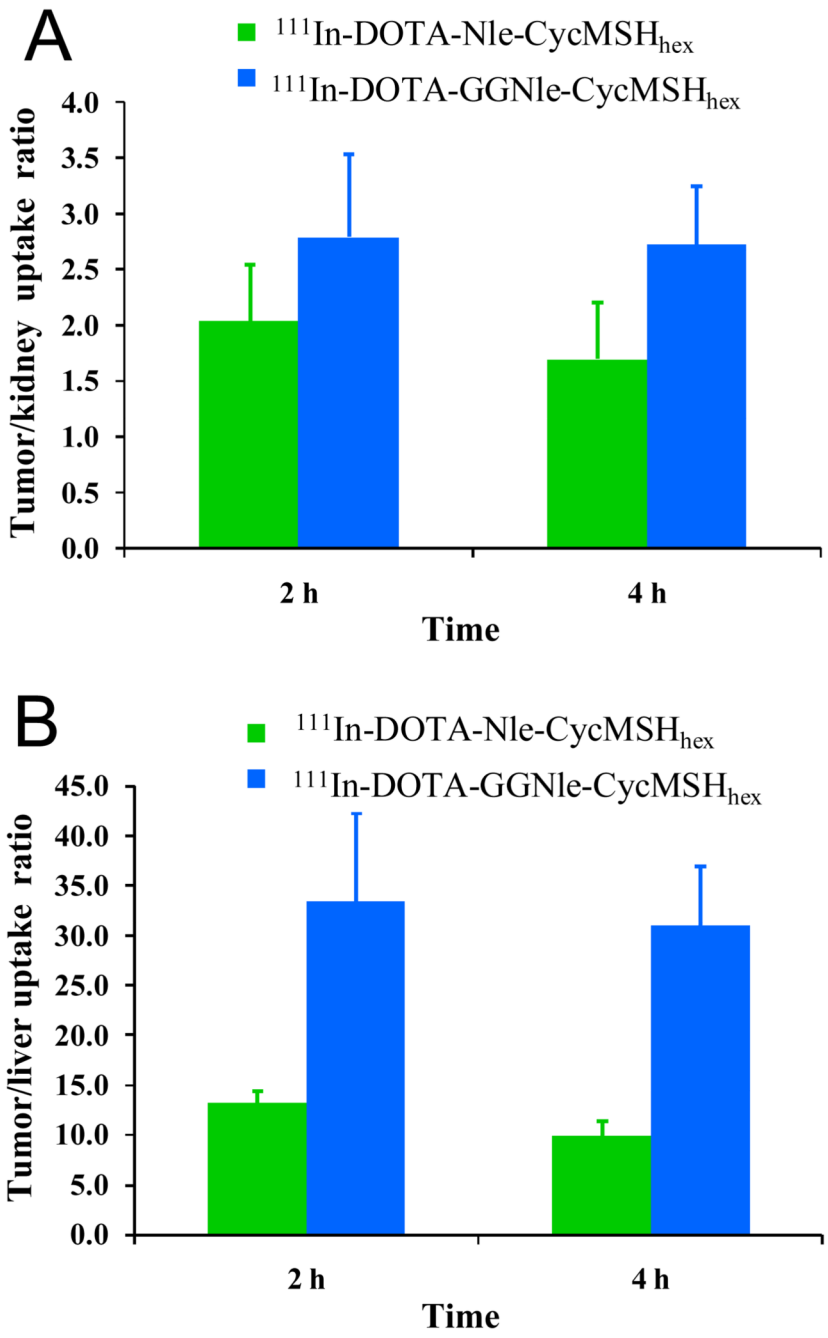

Figure 6.

The tumor/kidney (A) and tumor/liver (B) ratios of ^{111}In-DOTA-Nle-CycMSH$_{hex}$ (■) and ^{111}In-DOTA-GGNle-CycMSH$_{hex}$ (■) at 2 and 4 h post-injection. The data of ^{111}In-DOTA-Nle-CycMSH$_{hex}$ was cited from the reference [19] for comparison.

Table 1

DOTA-conjugated lactam bridge-cyclized alpha-MSH peptides.

	DOTA-Nle-CycMSH$_{hex}$	**DOTA-GGNle-CycMSH$_{hex}$**	**DOTA-GENle-CycMSH$_{hex}$**	**DOTA-NleGE-CycMSH$_{hex}$**
Amino acid linker between DOTA and the cyclic peptide moiety	-Nle-	-Gly-Gly-Nle-	-Gly-Glu-Nle-	-Nle-Gly-Glu-
Calculated molecular weight (Da)	1368.5	1482.6	1554.6	1554.6
Found molecular weight (Da)	1368.2	1482.0	1554.0	1554.0
Molecular Formula	$C_{64}H_{93}N_{19}O_{15}$	$C_{68}H_{99}N_{21}O_{17}$	$C_{71}H_{103}N_{21}O_{19}$	$C_{71}H_{103}N_{21}O_{19}$
MC1R binding affinity (nM)	1.8	2.1	11.5	873.4
HPLC retention time (min)	14.3	14.8	15.4	9.6
HPLC retention time for ^{111}In-conjugate (min)	10.7	17.7	21.7	N/A

The data of DOTA-Nle-CycMSH$_{hex}$ was cited from the reference [19] for comparison.

Table 2

Biodistribution of ^{111}In-DOTA-GGNle-CycMSH$_{hex}$ and ^{111}In-DOTA-GENle-CycMSH$_{hex}$ in B16/F1 melanoma-bearing C57 mice. The data were presented as percent injected dose/gram or as percent injected dose (mean ± SD, n=5)

	^{111}In-DOTA-GGNle-CycMSH$_{hex}$				**^{111}In-DOTA-GENle-CycMSH$_{hex}$**			
Tissues	**0.5 h**	**2 h**	**4 h**	**24 h**	**0.5 h**	**2 h**	**4 h**	**24 h**
				Percent injected dose/gram (%ID/g)				
Tumor	18.39±2.22	19.05±5.04	18.6±3.56	6.77±0.84	11.75±2.00*	8.99±1.91*	5.3±2.84*	4.40±0.87*
Brain	0.21±0.18	0.03±0.03	0.04±0.03	0.01±0.01	0.07±0.01	0.02±0.01	0.04±0.04	0.03±0.01
Blood	3.17±0.45	0.12±0.11	0.01±0.01	0.02±0.01	1.28±0.09	0.16±0.05	0.14±0.06	0.01±0.01
Heart	1.35±0.26	0.24±0.12	0.01±0.02	0.01±0.01	0.66±0.17	0.06±0.04	0.06±0.04	0.06±0.02
Lung	2.97±0.71	0.28±0.07	0.13±0.10	0.07±0.05	1.31±0.29	0.31±0.14	0.20±0.04	0.12±0.05
Liver	1.41±0.22	0.57±0.09	0.60±0.03	0.60±0.10	0.67±0.17	0.50±0.12	0.36±0.03	0.26±0.01
Spleen	0.93±0.37	0.17±0.06	0.15±0.10	0.12±0.13	0.54±0.13	0.24±0.11	0.19±0.10	0.14±0.01
Stomach	2.18±0.28	1.30±0.12	1.14±0.13	1.17±0.48	0.95±0.15	0.28±0.03	0.49±0.14	0.41±0.01
Kidneys	15.19±2.75	6.84±0.92	6.82±1.19	5.44±1.58	9.06±2.20*	5.54±0.63*	6.25±0.51	4.21±0.03
Muscle	0.37±0.26	0.01±0.01	0.02±0.02	0.02±0.01	0.32±0.09	0.06±0.03	0.11±0.05	0.09±0.01
Pancreas	0.99±0.27	0.23±0.12	0.14±0.06	0.10±0.01	0.40±0.08	0.12±0.10	0.13±0.08	0.15±0.04
Bone	0.59±0.39	0.10±0.09	0.10±0.08	0.04±0.04	0.13±0.10	0.08±0.05	0.02±0.01	0.06±0.01
Skin	2.16±1.28	0.27±0.12	0.27±0.28	0.26±0.08	1.63±0.43	0.37±0.11	0.12±0.10	0.16±0.13
				Percent injected dose (%ID)				
Intestines	1.65±0.26	1.30±0.32	0.97±0.38	0.74±0.13	0.95±0.14	0.68±0.26	1.45±0.85	0.76±0.45
Urine	60.80±4.05	88.46±1.75	88.39±3.06	93.23±1.60	83.56±0.49	89.65±6.24	91.38±1.85	93.57±0.12
				Uptake ratio of tumor/normal tissue				
Tumor/Blood	5.80	158.75	1860.00	338.50	9.18	56.19	37.86	440.00
Tumor/Kidneys	1.21	2.79	2.73	1.24	1.30	1.62	0.85	1.05
Tumor/Lung	6.19	68.04	143.08	96.71	8.97	29.00	26.50	36.67
Tumor/Liver	13.04	33.42	31.00	11.28	17.54	17.98	14.72	16.92
Tumor/Muscle	49.70	1905.00	930.00	338.50	36.72	149.83	48.18	48.89
Tumor/Skin	8.51	70.56	68.89	26.04	7.21	24.30	44.17	27.50

* $P<0.05$, significance comparison in tumor and kidney uptakes between ^{111}In-DOTA-GGNle-CycMSH$_{hex}$ and ^{111}In-DOTA-GENle-CycMSH$_{hex}$.